Chemiresistive Sensor Array from Conductive Polymer Nanowires Fabricated by Nanoscale Soft Lithography

Yang Jiang,[a] *Ning Tang,* [a] *Cheng Zhou,* [a] *Ziyu Han,* [a] *Hemi Qu**[a] *and Xuexin Duan,* *[a]

[a] State Key Laboratory of Precision Measuring Technology & Instruments, College of Precision Instrument and Opto-electronics Engineering, Tianjin University, Tianjin 300072, China.

1. EXPERIMENT

1.1 Composite Flat PDMS Substrates

The flat PDMS substrates were first composite by casting the liquid prepolymer of the PDMS base and the curing agent in a 10:1 (w/w) ratio onto a silicon wafer which an anti-adhesion layer (1H,1H,2H,2H-Perfluordecyltrichlorosilane) had been deposited. After degassing to remove air bubbles, a piece of cover glass (10mm×10mm) which has been cleaned using piranha solution (3:1 mixture of sulfuric acid and hydrogen peroxide. CAUTION! Piranha solution should be treated with great care in open containers in a fume hood. Piranha is high corrosive and toxic and potentially explosive) was put into the uncured mixture. The glass sank to the bottom of the PDMS liquid leaving a thin layer between the glass and the silicon wafer. After curing at 80℃ for 2 hours, the flat PDMS was cooled to room temperature and peeled off from the silicon wafer.

1.2. NIL Procedure

Before spin-coating the resist, the composite PDMS substrate was ultrasonically cleaned by ethanol solution for 5min. A thin film of mr-I T85 solution was spin-coated onto the substrate, followed by a soft baking step at 140℃ for 2min in a hot oven.

The imprint template consist of silicon nanoridges with 60nm in width and 80nm in height. 1H,1H,2H,2H-Perfluordecyltrichlorosilane was then used as an anti-adherent layer to facilitate the separation between the template and substrate.

A composite PDMS substrate coated with mr-I T85 and silicon template were inserted into a stamping machine (769YP-30T) and the temperature was raised to 135℃. Then, 2 bar of pressure was applied to the system for 40s. Upon cooling to 65℃, the template was separated from the PDMS substrate.

1.3. Pattern Transfer

After NIL procedure, a short oxygen plasma step (10mTorr; 10W; 10sccm O_2; 15s) was used to substrate surface to promote adhesion. Subsequently, the PDMS mold was placed in contact with a substrate, which has a 300nm thick SiO_2 layer formed on a silicon substrate as an insulating layer, so that the grooves forms channels (capillaries). At the edges of the nanochannels, a few drops of water were applied immediately for good sealing. The water filling the channels generates a negative pressure and thereby assists the sealing.

After water evaporation, the PEDOT: PSS solution was dropped at the open end of the PDMS mold; the liquid spontaneously filled the channels under the effect of capillary pressure. Hereafter, the sample was left for the solutions to dry out. After the solvent completely evaporated, the PDMS mold was gently removed from the patterns on the substrate surface.

1.4. Contact Pad Fabrication

After PEDOT:PSS nanowires were fabricated on the substrate, the electrodes were prepared by the standard MEMS (Micro-Electro-Mechanical-Systems) procedure. 50nm thick chromium and 120nm thick gold layers were deposited by thermal evaporation.

1.5. Surface-to-volume ratios

The surface to volume ratio is conventionally written as $R = S / V$, for PEDOT: PSS nanowires (PPNWs), where

$$S_{\mathrm{PPNWs}} = (1+L/\delta) \times (2HL+WL+2WH), \qquad (1)$$

$$V_{\mathrm{PPNWs}} = HWL \times (1+L/\delta), \qquad (2)$$

For nanofilm, where

$$S_{\text{nanofilm}} = L^2 + 4LH, \tag{3}$$

$$V_{\text{nanofilm}} = HL^2. \tag{4}$$

Here, L is the length of the standard area, δ is the space between nanowires, H is height of the single nanowire and the nanofilm, W is the width of the single nanowire.

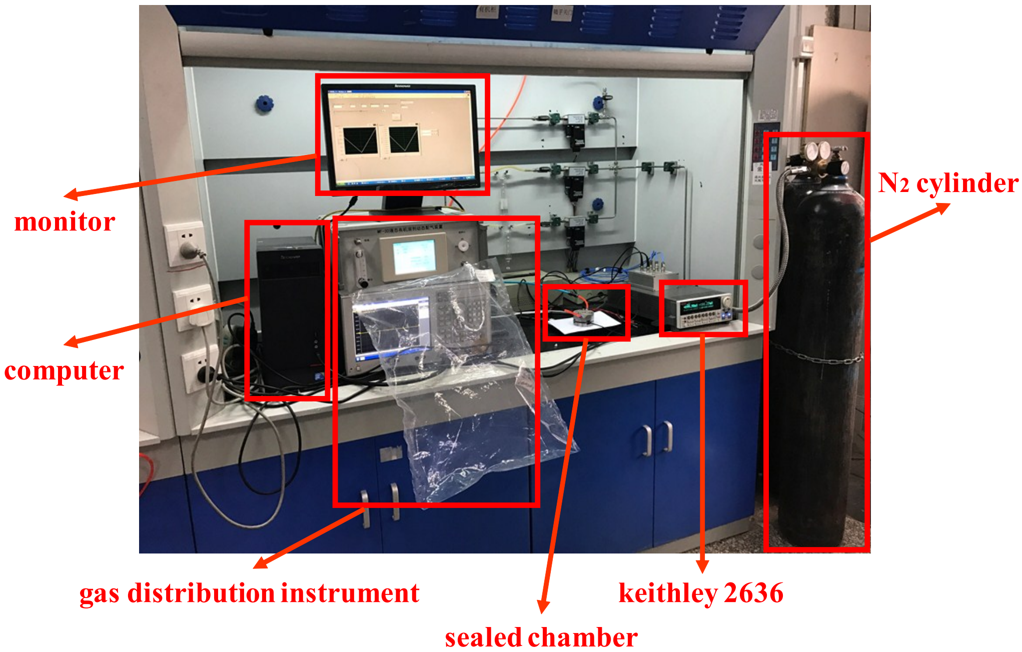

Fig. S1 Schematic of the overall gas delivery system.

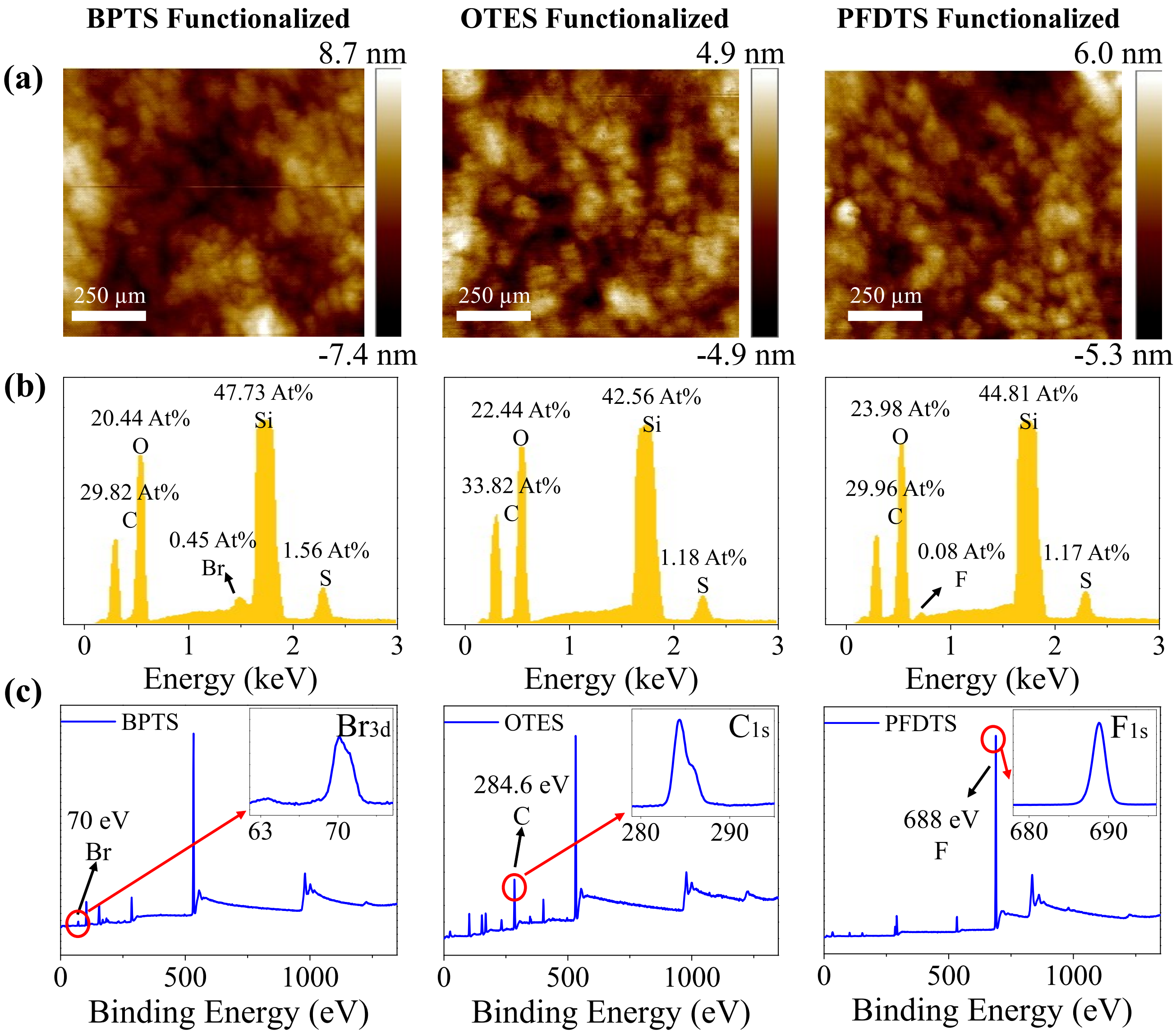

Fig. S2 Characterization of the SAMs functionalized PEDOT: PSS. (a) The atomic force microscopy of the BPTS, OTES and PFDTS functionalized PEDOT: PSS. (b) Energy-dispersive X-ray spectrum of the BPTS, OTES and PFDTS functionalized PEDOT: PSS. (c) X-ray photoelectron spectroscopy of the BPTS, OTES and PFDTS functionalized PEDOT: PSS.[1-3]

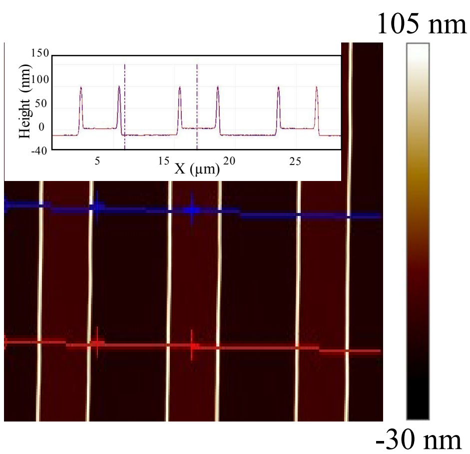

Fig. S3 AFM height image (22 μm × 20 μm) of the nanoimprint mold and its corresponding cross-sectional profile.

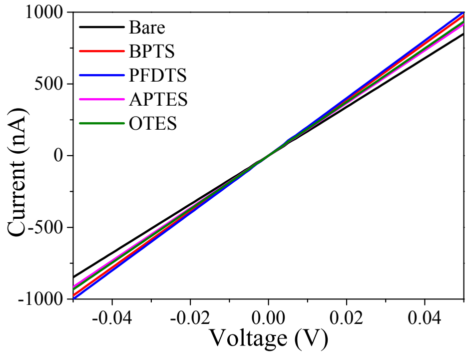

Fig. S4 I−V characteristics of the five nanowires chemiresistors.

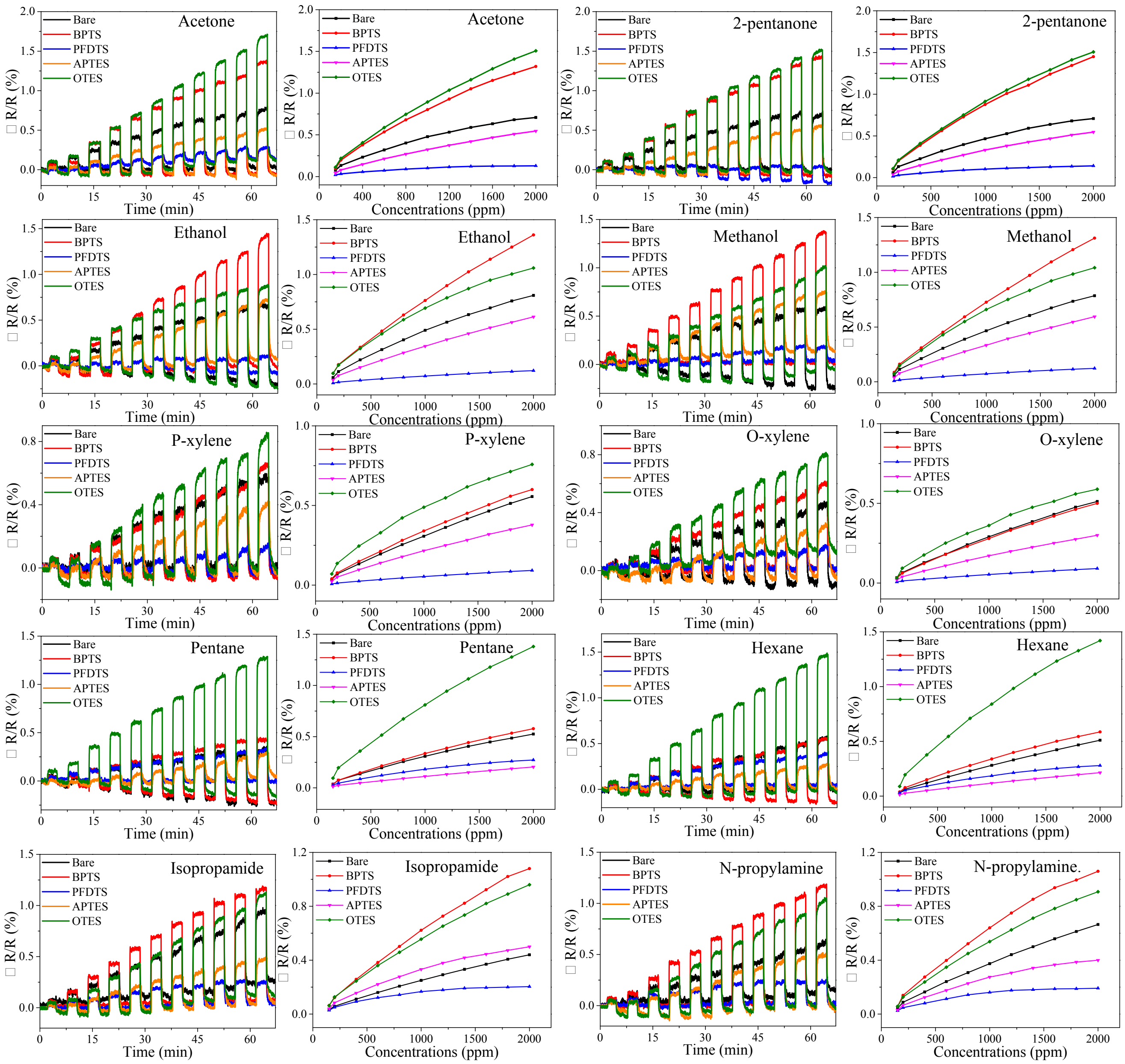

Fig. S5 Transient response−recovery characteristics, real-time responses on periodic exposure and changes in responses as a function of the VOCs concentration

Table S1 The sensitivity and LOD of the chemiresistors to all the analytes

	LOD (ppm)					Sensitivity (10^{-4}/ ppm)				
	Bare	BPTS	PFDTS	APTES	OTES	Bare	BPTS	PFDTS	APTES	OTES
acetone	35.25	19.54	162.66	49.88	18.10	5.19	9.37	1.13	3.67	10.11
2-pentanone	33.40	18.48	145.10	49.31	17.86	5.38	9.90	1.26	3.71	10.25
methanol	34.74	23.24	221.79	49.02	24.02	5.27	7.87	0.83	3.73	7.62
ethanol	33.30	22.08	216.31	47.03	23.54	5.50	8.29	0.85	3.89	7.77
pentane	54.05	47.85	89.21	147.81	20.57	3.39	3.82	2.05	1.24	8.90
hexane	58.94	47.15	87.64	139.85	18.84	3.11	3.88	2.09	1.31	9.71
o-xylene	53.33	49.46	304.46	74.28	33.24	3.43	3.70	0.60	2.46	5.51
p-xylene	57.84	57.11	311.79	95.32	39.87	3.16	3.20	0.59	1.92	4.59
n-propylamine	66.68	26.36	90.48	47.55	28.85	2.74	6.94	2.02	3.85	6.34
isopropylamine	43.56	25.29	99.08	59.08	29.68	4.20	7.23	1.85	3.10	6.17

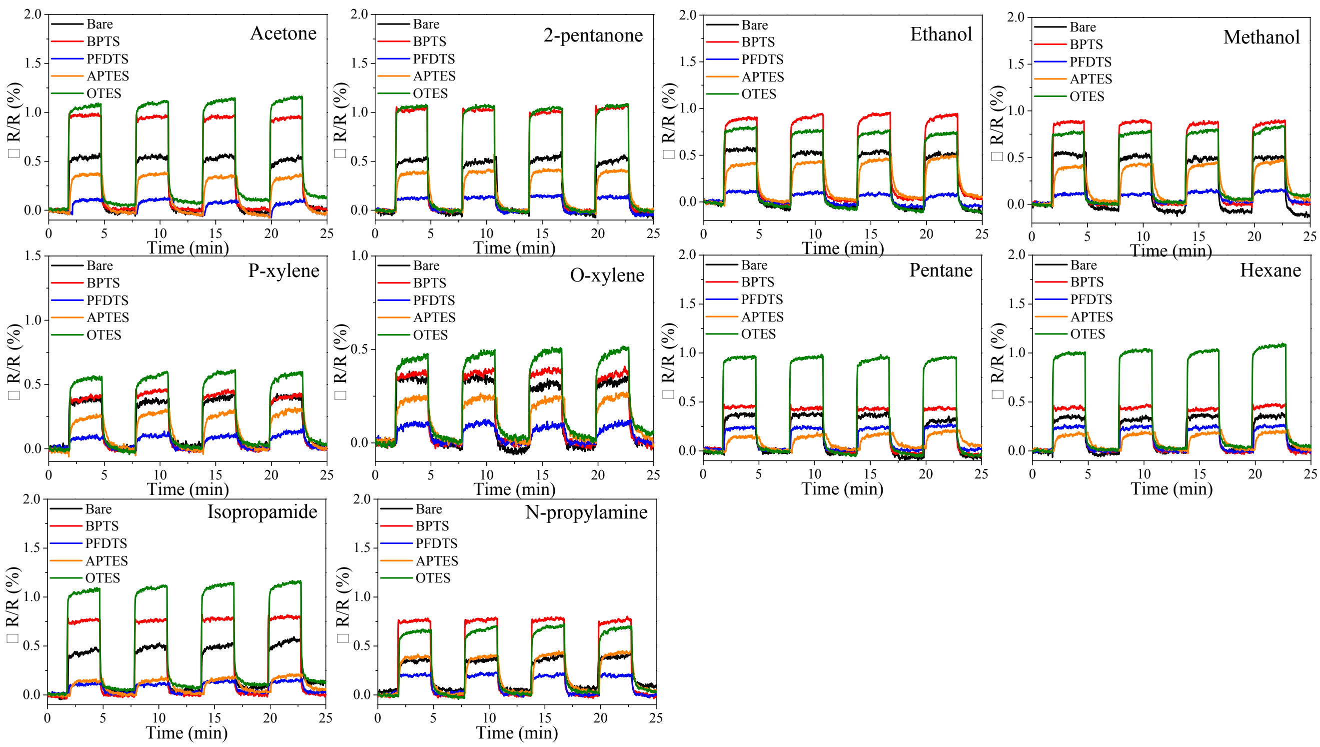

Fig. S6 Repeatability test of the chemiresistor gas sensors towards VOCs at 1000 ppm.

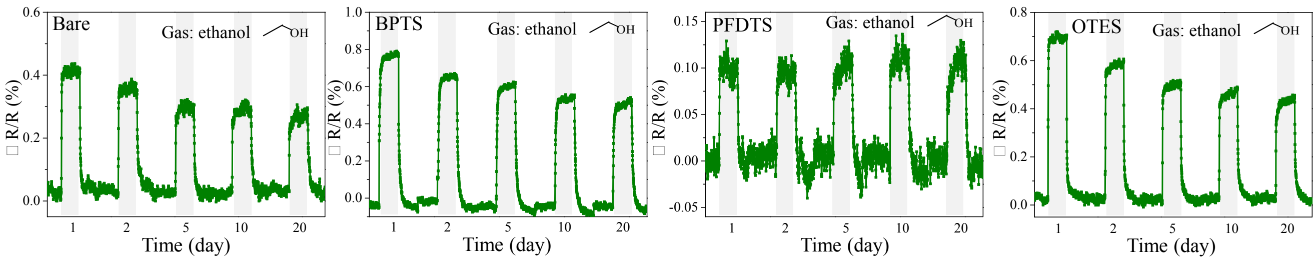

Fig. S7 Long-term stability detection of the chemiresistors exposed to ethanol.

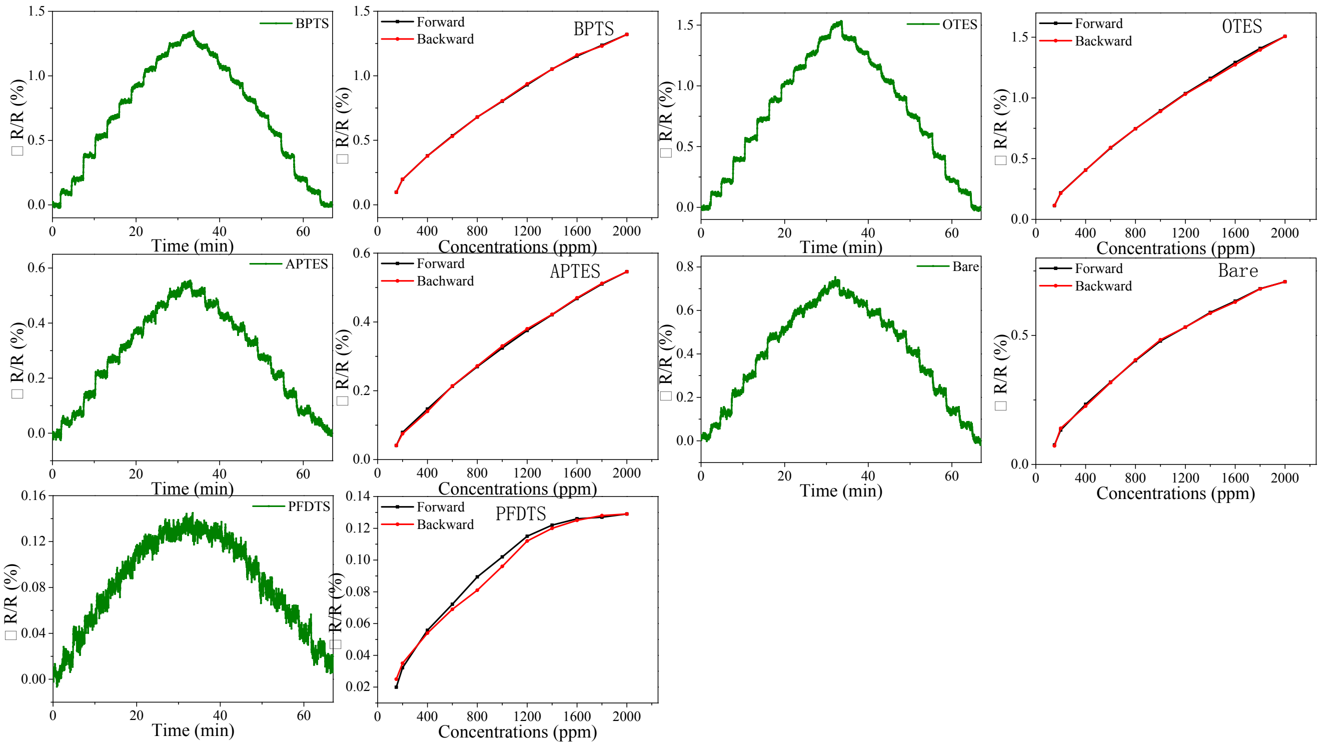

Fig. S8 Performance of the five PEDOT: PSS nanowire chemiresistors in a hysteresis cycle

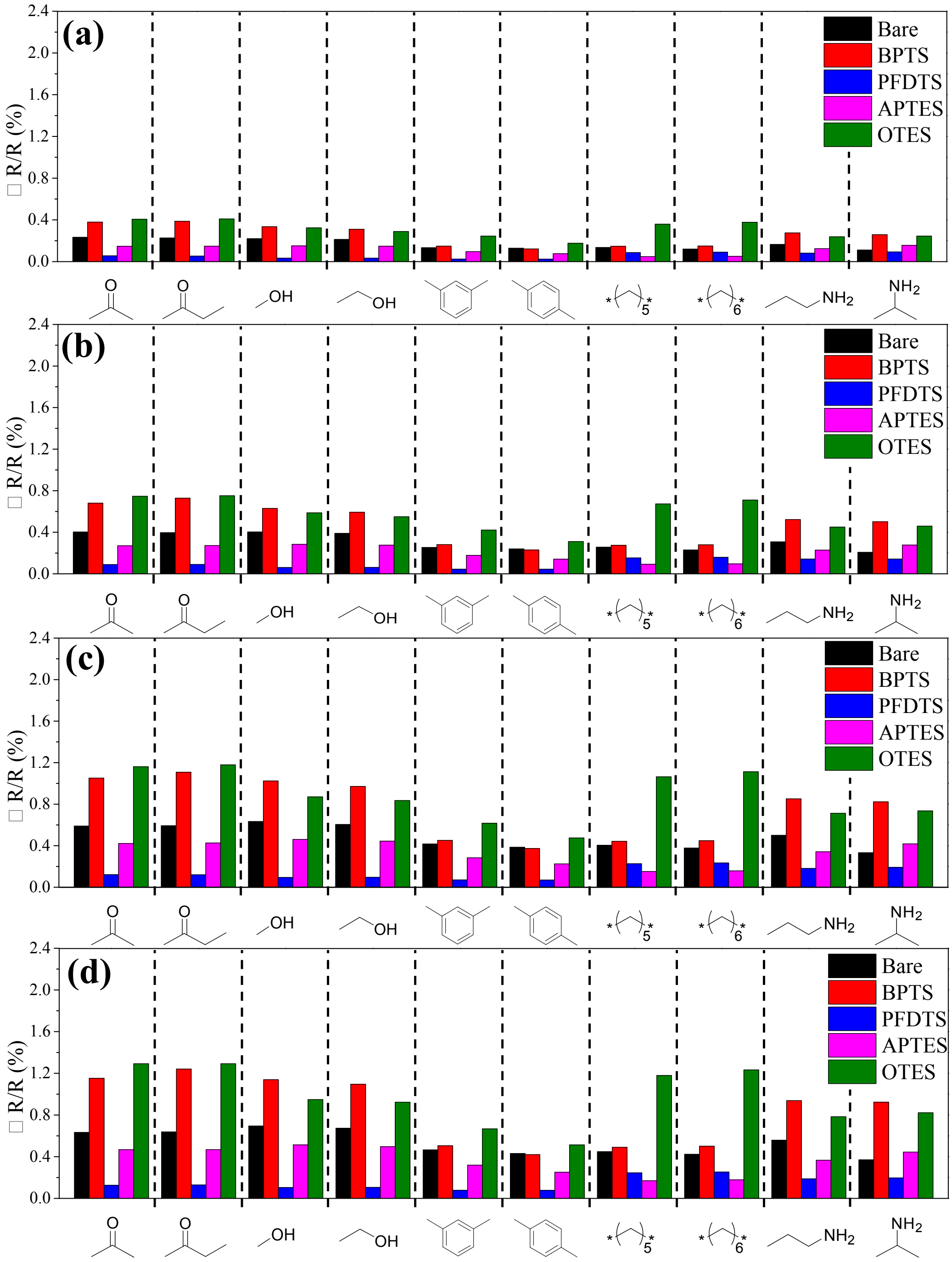

Fig. S9 Responses of PEDOT: PSS nanowires chemiresistive gas sensors functionalized by different SAMs at (a) 400 ppm, (b) 800 ppm, (c) 1200 ppm and (d) 1600 ppm.

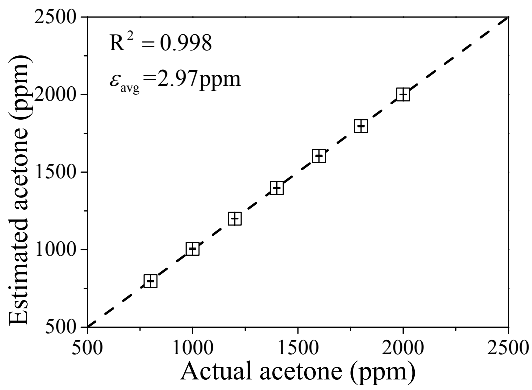

Fig. S10 Sensor array's estimation of acetone concentration against the actual level by multivariate linear regression.

Table S2 The function coefficients of the multivariate linear regression in the single analysis

VOCs	Coefficients			
	constant	PC1	PC2	ε (ppm)
acetone	3047.001	1196.207	-486.340	2.97
pentanone	-899.623	1147.730	-3182.610	21.94
ethanol	-521.974	538.372	-1358.796	6.35
methanol	-69.295	556.781	-1070.977	4.35
p-xylene	795.143	1362.734	-2138.122	7.47
o-xylene	139.881	1106.901	-2124.577	6.56
pentane	3488.973	1437.001	-691.232	4.46
hexane	3047.001	1196.207	-486.340	2.97
isopropamide	1714.007	818.361	-649.136	10.89
n-propylamine	1512.623	766.008	-829.694	17.23

Table S3 The function coefficients of the linear discrimination analysis

Fisher's Classification Function Coefficients															
	group														
	1	2	3	4	5	6	7	8	9	10	11	12	13	14	15
Bare	-2.792	-26.633	20.756	14.309	55.788	46.649	-55.939	-78.656	-178.759	-44.007	-2.792	-26.633	20.756	14.309	55.788
BPTS	-.461	86.791	14.409	23.318	-95.973	-139.075	20.467	24.273	103.203	156.287	-.461	86.791	14.409	23.318	-95.973
PFDTS	-14.556	9.456	.814	5.103	-16.666	-27.570	83.821	95.793	137.330	91.616	-14.556	9.456	.814	5.103	-16.666
APTES	-2.595	-45.825	2.780	-2.407	39.638	72.247	-8.849	1.505	59.636	-63.431	-2.595	-45.825	2.780	-2.407	39.638
OTES	36.103	-1.677	-26.295	-27.251	18.606	47.313	-16.535	-19.343	-102.560	-115.777	36.103	-1.677	-26.295	-27.251	18.606
constant	-19.928	-27.556	-20.681	-18.192	-22.078	-30.487	-76.976	-90.035	-126.694	-67.458	-19.928	-27.556	-20.681	-18.192	-22.078

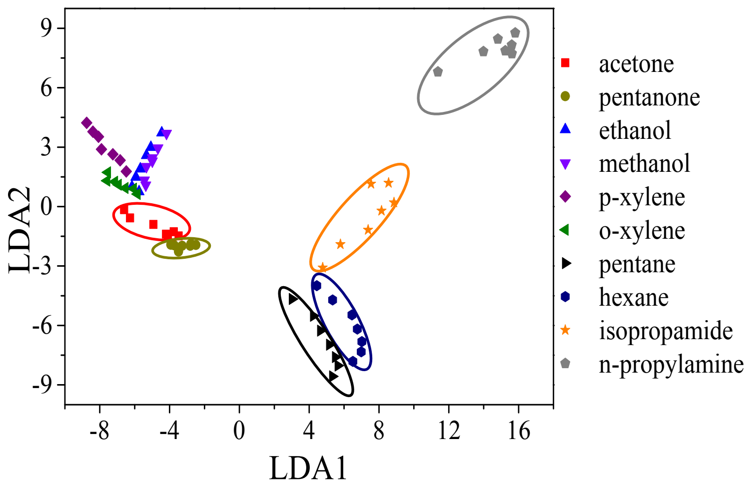

Fig. S11 LDA score plot of the first 2 discriminant factors (LDA1 and LDA2) achieved for the sensor array to ten VOCs.

Table S4 The testing individual ethanol and hexane concentrations and their binary mixtures concentrations

	individual		Binary mixture	
	ethanol	hexane	ethanol	hexane
Concentration (ppm)	800	800	800	800
	1000	1000	800	1200
	1200	1200	1200	1200
	1400	1400	1200	8000
	1600	1600	1600	8000
	1800	1800	1600	1600
	2000	2000		

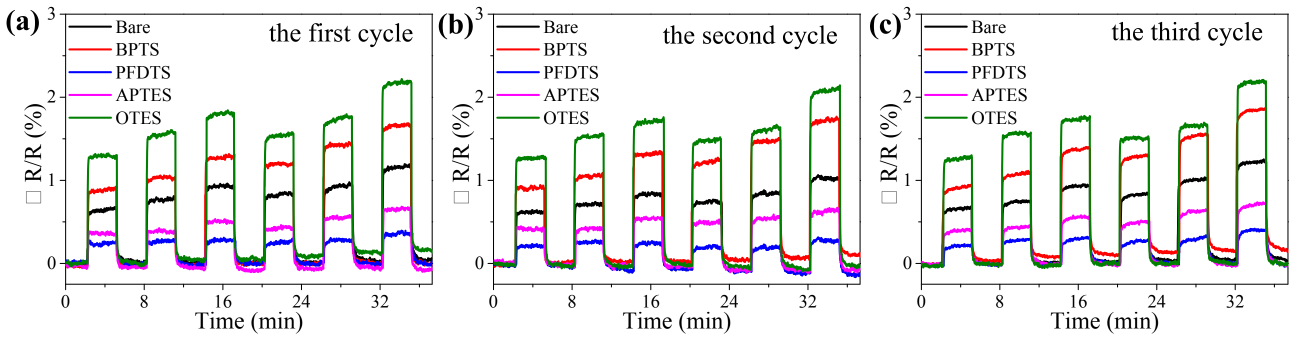

Fig. S12 Responses of PEDOT: PSS nanowires chemiresistive gas sensors to different binary vapor combinations in three cycles.

REFERENCE

1. X.-L. Zhou, F. Solymosi, P. Blass, K. Cannon and J. White, *Surface Science*, 1989, **219**, 294-316.
2. J.-S. Kim, H.-W. Yoo, H. O. Choi and H.-T. Jung, *Nano letters*, 2014, **14**, 5941-5947.
3. M. D. DUCA, C. L. PLOSCEANU and T. POP, *Journal of applied polymer science*, 1997, **67**, 2125-2129.